ISSN 0252-1075
Contribution from IITM
Research Report No. RR-111

Diagnostic Analysis of Wintertime Rainfall Events over the Arabian Region

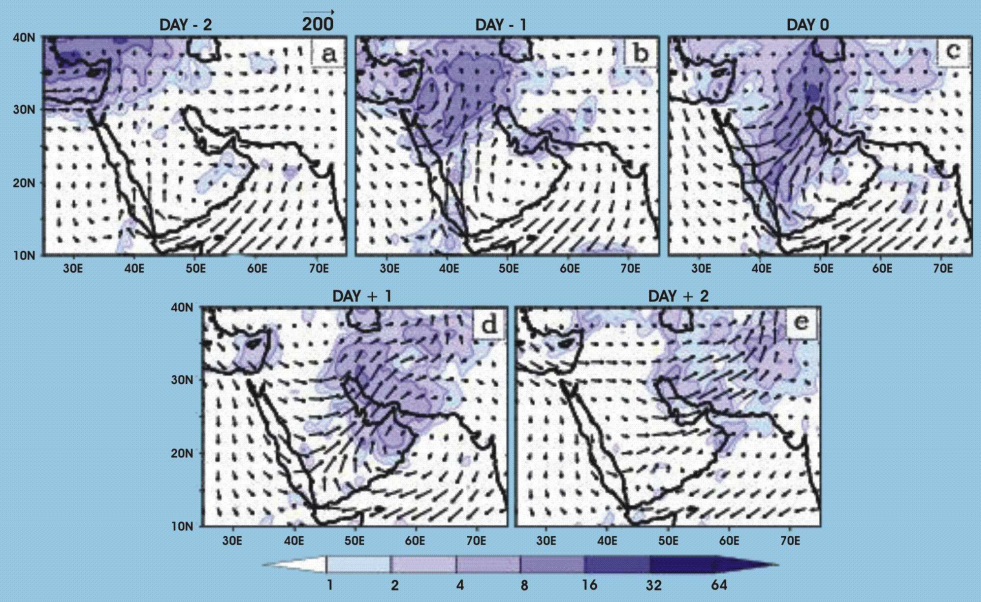

Milind Mujumdar

April 2006

Indian Institute of Tropical Meteorology
Pune - 411 008, India

ISSN 0252-1075
Contribution from IITM
Research Report No. RR-111

Diagnostic Analysis of Wintertime Rainfall Events over the Arabian Region

MILIND MUJUMDAR

APRIL 2006

Indian Institute of Tropical Meteorology
Dr. Homi Bhabha Road, Pashan Pune - 411 008
Maharashtra, India

E-mail : lip@tropmet.res.in Fax : 91-020-25893825
Web : http://www.tropmet.res.in Telephone : 91-020-25893600

Diagnostic analysis of wintertime rainfall events over the Arabian region

Milind Mujumdar [1, 2]

Abstract

Wintertime weather disturbances over the Saudi Arabian region are diagnosed using observations and reanalysis data. Wintertime rainfall events over Arabian Peninsula are associated with southeastward propagating weather systems from the Mediterranean region as a couplet of high and low. The weakening of vertical wind shear in the westerly jet-stream is an influential factor in modulating the upper tropospheric divergence and the reinforcement of lower tropospheric convergence. An elongated cyclonic circulation over the southwest Saudi Arabia enhances moisture transport from the Red Sea to southern Saudi Arabian region. Longitude-pressure cross sections of vorticity budget analysis of the Arabian weather events reveal that vortex-stretching term mainly contributes to the vorticity generation over Arabian region during wintertime rainfall events, with secondary contributions from zonal and meridional advection terms as well as the tilting term. During the day of significant rainfall events these transient weather disturbances intensify and organize over Arabian Peninsula and subside towards east of Arabia, while propagating eastward. These wintertime weather disturbances are helpful in understanding the duel character of tropical and extra-tropical systems in causing weather over the Arabian region.

---

[1] *Indian Institute of Tropical Meteorology, Pune, India.*

[2] *Affiliated with Global Hydrological Project Laboratory, Nezu, Tokyo and Department of Earth and Planetary Science, Graduate School of Science, University of Tokyo, Tokyo, Japan.*

E-mail: mujum@tropmet.res.in

Introduction

Wintertime rainfall is crucial for the copious population spread around one of the largest sand deserts over the Arabian Peninsula. The wintertime rainfall exert profound impact on the water management to meet the urban, industrial and agricultural need, which is carried out through recently established network of dams, along with the other water resources, like underground aquifers and desalination plants. The mountainous regions Asir and Hezaj province along the Red sea coast and the mountains of Yemen and Oman, rising to the height of 2.5Km to 3.5 Km, receives periodic monsoon-like downpours and an annual rainfall of about 400 mm (Columbia Electronic Encyclopedia, www.cc.columbia.edu/cu/cup/ and National Climatic Data Center, USA). While, across the mountains the rainfall is low and unreliable; below 200 mm and often less than 100 mm, over basin-shaped interior consisting of alternating steppe and desert landscape making it so arid (Sen, 1983, Nouh, 1987, Bazuhair et al. 1997). During the peak of the winter season around January the mid-latitude frontal systems reach its southern most latitude around Mediterranean Sea region (Trigo et. al. 2002). Recent study of tropospheric moisture budgets over the peninsular region of Saudi Arabia (Chakraborty et. al. 2006) also shows strengthening of moisture supply over the region during winter season. The rainfall over most of the Arabian region is generally restricted to a few wet spells, brought by weather disturbances originating over the Mediterranean Sea, during winter season.

There are numerous theoretical, statistical and observational studies that have enhanced our understanding in weather disturbances following the wave guide over Mediterranean and adjacent regions in the past few decades (Reiter, 1975, Hoskins and Pedder, 1980, Mayengon 1984, Radinoivic 1987, Lee et. al. 1988, Bazuhair et al., 1997, Trigo et. al., 2002). The record-breaking precipitation in summer of 2002 in Europe has renewed the interest; it appears to be due to anomalous vorticity transport in the upper troposphere associated with Rossby wave propagation as well as anomalous surface conditions (Nakano 2004). However, little attention has been paid to the dynamics of southeastward propagating frontal system in the Middle East located down stream of Mediterranean. The rainfall associated with those weather disturbances is very important in the Arabian Peninsular region from a socioeconomic viewpoint. The classical extra-tropical transition of tropical remnants has been well discussed by the researchers (Ritchie and Elsberry 2001, Kelin et. al. 2002, Mc Toggart-cowan et. al. 2004), however it would be more exciting to explore the influence of wintertime

mid-latitude system in contributing to the wide spread rainfall over Arabian Peninsula. Thus the primary objective of this study is to describe the dynamical characteristics of the spatiotemporal evolution of wintertime weather disturbances over the Saudi Arabian region using available datasets.

Data sets

The diagnostic analysis is carried out using several observed data sets from multiple sources. The Global Precipitation Climatology Project's (GPCP, see *http://precip.gsfc.nasa.gov/gpcp_daily_comb.html*) daily rainfall data set is used for detailed analysis of the evolution of the large scale rainfall events for the period 1997-2002. These global 1^0x1^0 daily rainfall estimates are based on gauge and satellite observations. The daily atmospheric data such as wind, surface pressure, moisture, vertical velocity, geopotential height, and temperature are obtained from the National Center for Environmental Prediction-National Center for Atmospheric Research (NCEP-NCAR) reanalysis dataset (Kalnay et al., 1996). Besides these gridded variables, *in situ* rainfall data archived by Ministry for Environmental Protection in the Kingdom of Saudi Arabia. The surface climate summaries over Middle East (see *http://www.ncdc.noaa.gov/oa/climate*) prepared by US Navy, Air Force and National Climate Data Center (NCDC) are also utilized to validate the analyses.

Origin of the synoptic weather disturbances

The daily rainfall distribution is analyzed over the Arabian region and its neighborhood during winter season to identify significant rainfall events over the region. Visual examination of the GPCP data showed two active rainfall regions around Mecca of the Province of Asir and around Basra located near the northern edge of Persian Gulf respectively. Both Mecca and Basra regions have a number of rain gauge stations, which provide better ground truth for the satellite data. When the rainfall, over Mecca (around 20^0N, 42^0E) and Basra (around 30^0N, 47^0E) regions, exceeds a threshold value of 5 mm/day within a grid box of 5^0 latitude by 5^0 longitude, i.e. one standard deviation of the wintertime rainfall, the rain event is considered as a significant weather event. A slight change in the location of grid box does not influence the Arabian rainfall events. We thus identify 19 Arabian rainfall events, during the months of January, February and March for the period ranging from 1997 through 2002 (Table 1). The number of events is enough for statistical significance of the present analysis.

Table 1. Wintertime Arabian rainfall events

	1997	1998	1999	2000	2001	2002
January	7th and 15th	4th and 5th	8th and 15th	5th	8th	6th
February		11th				24th
March	5th and 22nd	17th and 29th	28th	-	3rd and 19th	17th

In order to examine the spatial distribution of significant rainfall events we have prepared composite maps based on the identified significant rainfall events during January, February and March as listed in Table 1. The evolution of the weather event is examined by extending the composite analysis to days prior and after the occurrence of significant rainfall events on Day 0. The composites preceding the Day 0 are given as Day -1, Day -2 and those following the Day 0 are noted as Day +1, Day +2. Figure 1a shows the heavy precipitation area around the Mediterranean region during Day -2. The precipitation area moves southeastward from Day -2 and covers the northern part of the Red Sea and adjacent continental Arabia on Day -1. On Day 0, the rainfall area extends from the Red Sea adjacent to Mecca to the southern part of the Caspian Sea (Figure 1c). Two rainfall maxima are found over the region of our analysis: the major maximum one over Basra and a minor maximum one over Mecca. The major maximum, which lies to the west of the mountainous region of Iran, is stronger and well spread as compared to the minor one that lies near Mecca. It is noteworthy that the strong precipitation over Basra is established one day prior (on Day -1) to significant rainfall over Mecca. Following the Day 0 event, convective activity becomes weaker in strength and moves northeastward over the high altitude regions of Iran on Day +1 (Figure 1d) and continues to move eastward during Day +2 (Figure 1e), covering parts of northwest India.

The composites in March for Day 0 event (Figure 2) exhibit a striking similarity in the spatial distribution of rainfall as compared to those in January shown in Figure 1c. However, it is noted that the east-west extent is narrower in March as compared to that in January. The amplitudes of rainfall maxima are also weaker in strength during March for Day 0 event.

The time sequence of moisture transport vector ($\vec{Q}$) exhibiting the moisture convergence from the Oceanic areas into Arabian region is also illustrated in Figure 1 (a-e). Here moisture transport vector $\vec{Q}$ (units: Kg m^{-1} s^{-1}); $\vec{Q} = \frac{1}{g}\int_{P_u}^{P_s} q\,\vec{V}\,dP$, where g is the acceleration due to gravity and q is the specific humidity; P_u is 300 hPa and P_s is the surface pressure over a given geographical location; is computed from NCEP data. The moisture convergence over the Mediterranean Sea and the adjoining area on Day –2 is consistent with the strong rainfall pattern over the region (Figure 1a). A conspicuous feature on Day -1 is the band of elongated southeastward moisture influx over the Red Sea and the adjacent continental Arabia. The enhanced eastward moisture transport over the mountainous region of the Province of Asir and Arabian Peninsula on Day 0 is due to stronger convergence over the region around 20^{o}N, which leads to the significant rainfall event on Day 0 (Figure 1c). This is an important feature exhibiting the influence of tropical characteristics associated with the convection (Daggupaty and Sikka 1977, Davidson 1995). On Day +1 the moisture flux is further enhanced over the high altitude region of Iran and, on Day +2, the area of enhanced convection extends further eastward over northwest India.

The time sequence of vertical velocity field at 500 hPa is presented in Figure 3 (a-e) during Day-2 to Day+2. The statistical significance of patterns of mid-tropospheric vertical velocity was evaluated using 2-tailed Student's t-test. The regions where the composite mean is statistically significant are shaded (Figure 3 a-e). It is worth noticing that these transient disturbances propagate eastward as a couplet of positive and negative contours. The pattern of ascending motion over Mediterranean Sea on Day –2 is coherent with the strong precipitation emerging over the region (Figure 1a) while, the descending motion extends eastward over north Arabia during Day -2. Also seen from the Figure 3b are the two regions of maximum vertical velocity at 500 hPa coinciding with the elongated precipitation pattern around Red Sea and northeast Arabian region, one day prior (Day –1) to the significant rainfall event. In addition, the mid-tropospheric descending region is seen to the east of Persian Gulf extending over Iran during Day–1. Subsequently the southeastward movement of rising and sinking regions (Figure 3c) overlaps with the two peaks of significant rainfall event (Figure 1c) on Day 0. The peak over Asir province results from the strengthening of the convection in the south west quadrant of the Arabian weather disturbances as shown by (Daggupaty and Sikka 1977). Further, on Day +1 the rising and sinking patterns at 500 hPa (Figure 3d) extend east of the Iranian region and on Day +2, these mid-tropospheric patterns of rising and sinking motions (Figure 3e) advances eastward over northwest India. Further, the time

sequence of atmospheric circulation features suggest that the transient weather disturbances associated with the rainfall events starts from the Mediterranean region 2 days prior (Day -2) to the occurrence of the significant rainfall in Saudi Arabia and propagates southeastward. The northwesterly wind associated with these wintertime weather disturbances is called "*winter Shamal*". This horizontal scale of the synoptic weather disturbance is larger than 1000 km. Nevertheless this southeastward propagating synoptic scale system over Arabian region is weaker in magnitude as compared to the diagnostic analysis carried out for Mediterranean cyclone propagating over Middle-east region (e.g. Lee et. al. 1988; Holton 1992; Grotjahn 1996; Trigo et. al. 2002), and is yet to be explored. Therefore we focus our attention to diagnose the evolution of the wintertime weather disturbances over the Saudi Arabian region.

Dynamics of the weather disturbances

The diagnosis of the magnitude and aerial extent of different atmospheric parameters associated with the tropical synoptic disturbances have varying importance in different regions and at different levels. In this section the dynamics associated with the development and propagation of the Arabian weather disturbances is studied by analyzing vertical structure of a typical case. This case study is also complemented by composite analysis at later stage. The time sequence of latitude-height cross sections of zonally averaged divergences (over 35^{o}E and 45^{o}E), are shown in Figure 4(a-e) for a typical event of 8^{th} January 1999. The strong upper level divergence can be seen around Mediterranean region in association with strong lower tropospheric convergence during Day-2. The southward penetration of the upper tropospheric divergence and lower tropospheric convergence during Day-2 to Day 0 over Mecca region is noteworthy. The strengthening of the lower tropospheric convergence is an important aspect, which in association with upper level divergence helps in understanding the dynamics of significant rainfall (Figure 4c). This is also consistent with enhanced moisture convergence over Mecca region during Day 0 (Figure 1c). Later it is shown that the stretching term associated with horizontal divergence has significant contribution in the vorticity budget analysis over Mecca region (similar to Davidson, 1995; Grotjahn 1996). After the significant rainfall event on Day 0, while the weather system moves eastward during Day +1 and Day +2, the entire vertical section of the system weakens in strength (Figure 4d-e). The time sequence of vertical cross section of divergence for Day-2 to Day+2 prominently exhibits westward tilt with height. The above diagnosis illustrates that the typical rainfall event over Arabia is associated with the southeastward propagating synoptic scale system.

Previous studies have shown that the analysis of the vorticity equation provides insight into the dynamics of synoptic scale systems (Krishnamurti 1968; Holton and Colton 1972; Reed and Johnson 1974; Daggupaty and Sikka 1977; Bosart and Lin 1984; Davidson 1995, Grotjahn 1996). Here, we have carried out budget analysis based on the following vorticity equation for the typical rainfall event of 8th January 1999.

$$\frac{\partial \zeta}{\partial t} = -(\zeta + f)Div. - u\frac{\partial(\zeta + f)}{\partial x} - v\frac{\partial(\zeta + f)}{\partial y} - \omega\frac{\partial \zeta}{\partial p} - (\frac{\partial \omega}{\partial x}\frac{\partial v}{\partial p} - \frac{\partial \omega}{\partial y}\frac{\partial u}{\partial p}) + \text{diffusion} \qquad (1)$$

Local Tendency = Stretching + Zonal advection + Meridional advection + Vertical advection + Tilting + diffusion.

The longitude-height cross sections of all the terms which contribute to the vorticity generation are shown in Figures 5-10; meridionally averaged between 20^{o}N and 30^{o}N during Day –2 to Day +2. From the time evolution of the vorticity tendency, it is found that the term forms a couplet with positive (negative) tendency (Figure 5a-e) east (west) of the lower tropospheric cyclonic circulation between 30^{o}E and 50^{o}E. The moisture convergence and convection (Figure 1a-c) leads to enhance vertical velocity and low-level convergence generating the vorticity couplet. Following the formation of the couplet, the vertical velocity would amplify (weaken) in area with positive (negative) tendency. The system would then move following the track of relative vorticity amplification, which implies motion from west to east during Day –2 to Day +2. As seen in the plot major contributions for the vorticity tendency come from vortex stretching, horizontal advection and tilting terms. From a scale analysis of all terms in the vorticity equation (1) it is found that the role of planetary vorticity advection is negligible and does not make any significant contribution.

The longitude-pressure cross-sections of stretching term in Figure 6(a-e) exhibit the eastward moving couplet of negative and positive contours, prominently between 30^{o}E to 50^{o}E, through the event period from Day -2 to Day +2. The positive values of stretching term seems to favor the relative vorticity below the steering level and negative values of divergence opposes the relative vorticity above the steering level (Figure 6c) while its eastward propagation. This term is important from the point of view of baroclinic energy conversion (Grotjahn 1996). The pattern of the vorticity generation term reverses with height. The westward tilt in the vertical structure of the positive contours becomes well organized during the day of significant rainfall event (Day 0)

(Figure 6c). It is worth noticing that the stretching term is significantly positive in the lower troposphere over the longitudinal region of interest around 40^{o}E, while the negative values of stretching term can be seen in the upper troposphere during Day 0. The vertical structure of the stretching term weakens with negative contours in lower troposphere and positive contours in upper troposphere over 40^{o}E (Figure 6d and 6e), while its eastward movement during Day +1 and Day +2.

The decomposition of the horizontal advection of vorticity into zonal and meridional components is useful for bringing out their relative contributions in vorticity generation. The vertical cross sections of zonal advection during Day –2 to Day +2 in Figure 7 exhibit strong core of positive contours preceded by vertical distribution of weak negative zonal advection between 20^{o}E to 60^{o}E. The pattern of vertical cross section of zonal advection of vorticity is supportive of eastward propagation of the weather disturbance (Figure 7a-e). The zonal advection varies with height, having maxima in the upper troposphere and weakens towards lower troposphere.

The meridional advection of eastward propagating relative vorticity is strongly negative with maxima at the upper troposphere (Figure 8a-e), which suggests the influence of the upper level trough on the lower tropospheric boundary layer conditions during the weather event over Arabia. Similar to the zonal advection term, this term also shows weakening of magnitude and aerial extent during Day –2 to Day +2. It is to be noted that the distribution of the negative meridional advection of vorticity is stronger in strength and wide spread in the spatial direction and fully extending to lower tropospheric levels as compared to the other terms in vorticity equation (1). Therefore the contribution of the meridional advection term (Figure 8c) in vorticity equation is considerably dominant over the longitude of interest around 40^{o}E, in particular during the significant rainfall event.

Figure 9 and 10, show eastward moving couplet of negative and positive contours in the time sequence of vertical advection of vorticity and tilting term respectively during Day –2 to Day +2. It is interesting to note from time sequence of longitude-pressure cross sections that the contribution of the tilting term is significant as compared to weaker vertical advection. Also the order of the magnitude of tilting term is comparable with the stretching and horizontal advection terms. In particular, vertical structure of vertical advection of vorticity and tilting term (Figure 10c) is organized on the day of significant rainfall event over Arabia (Day 0). The maximum of synoptic scale

tilting term during Day 0 lies in the mid-troposphere coinciding with the large amplitude of vertical velocity (Figure 3c) (similar to Figure 4b, pg. 2851, Grotjahn 1996). The vertical structure of the vertical advection of vorticity and tilting term weakens, while depicting eastward movement during Day +1 and Day +2. The tilting term (Figure 10a-c) tends to modify vertical shear of the horizontal wind and thereby exerts the controlling influence on the vorticity changes in the middle troposphere (Davidson 1995, Grotjahn 1996).

The time sequence of vertical structure of weather disturbances over Arabian Peninsula differs from case to case. The variation of the location of centers of weather systems (Table 2) tend to amplify the variations among the vorticity equation terms involving products and derivatives for different cases with respect to different pressure levels. At a particular pressure level, the results of the diagnostic analysis from a typical case could be confirmed by performing composite analysis of similar cases. We have composited the data from each case (Table 2) for carrying out the vorticity budget analysis at 700 hPa during the significant rainfall event (Day 0). The original latitude-longitude grid point values of the wind components at 700 hPa for Day 0, were spatially shifted so as to place the center of weather disturbance in each case at (20^{o}N and 43^{o}E), a leeward location of the Mecca region of Asir province, which is also coherent with the center of the moisture convergence in Figure 1c.

Table 2. Location of center of Arabian weather disturbance, at 700 hPa during Day 0.

Case number	Date	Latitude (^{o}N)	Longitude (^{o}E)
1	07 January 1997	22.5	40.0
2	15 January 1997	20.0	45.0
3	04 January 1998	20.0	37.5
4	05 January 1998	17.5	40.0
5	08 January 1999	15.0	37.5
6	15 January 1999	22.5	45.0
7	05 January 2000	17.5	37.5
8	08 January 2001	15.0	45.0
9	06 January 2002	22.5	42.5

The composited wind divergence based on the shifted wind components at 700 hPa (Figure 11a-g) exhibits good agreement in capturing the horizontal convergence around 40^{o}E-50^{o}E, when compared with the lower tropospheric divergence field of a typical rainfall event as shown in Figure 11a during Day 0.

The spatial distributions of all the terms, which contribute to the vorticity budget, are shown in Figure 11 (a-e) during Day 0. The strong divergence (Figure 11a), stretching term (Figure 11c) meridional advection (Figure 11e) and tilting term (Figure 11g) turns out to be dominant in vorticity equation. The vorticity budget analysis of composite at 700 hPa (Figures 11a-g) turns out to be closer to that suggested by the typical case study (Figures 6-11). Following (Davidson 1995; Grotjahn 1996) it can be seen from the longitude-pressure patterns that the two fields have about as much reinforcement as they do cancellation (Figures 7 and 8). The meridional and zonal advection of vorticity is the classical example in this regard. Depending on amplitude, aerial extent and mutual interactions, the terms involved in vorticity equation can be qualitatively categorized into different categories. The stronger divergence and advection terms can be put in first category. The tilting term can be put in second category and the vertical advection can be put in the third category. The contribution of stretching term is significant, having large amplitudes in the lower as well as middle troposphere, over the Province of Asir and eastward Arabian Peninsula (consistent with the Davidson 1995). Weakening of the vertical wind shear of the transitioning Mid-latitude weather disturbance embedded into westerly jet-stream plays a crucial role in coupling the tropical moist convection. It is worth noticing the common characteristics of the wintertime weather disturbances over Arabia with the typical tropical systems such as banding structures and wide spread convection (Kein et al. 2000; Evans and Hart 2003).

Discussion and summary

Significant synoptic-scale wintertime rainfall events occur over Arabian Peninsula, a region of the world seldom afflicted by such wet spells. The total 19 wintertime rainfall events were identified over Arabian region. These southeastward propagating wintertime weather disturbances with a typical horizontal scale larger than 1000 km are traced back to the Mediterranean region. These transient weather disturbances move eastward as a couplet of a high followed by a low during Day –2 to Day +2. The elongated cyclonic circulation over northern part of Red Sea and adjacent

Arabian region transports moisture from Red Sea to large region of Saudi Arabia during (Day –1). The southeastward propagation of cyclonic system during the significant rainfall event (Day 0) enhances the moisture transport over mountainous region of province of Asir along the Red Sea and adjacent southern Saudi Arabian region. During the day of significant rainfall events (Day 0) these transient weather disturbances intensify and get organized over Arabian Peninsula. Following the Day 0 event, these transient synoptic systems become weaker in strength and moves northeastward over the high altitude regions of Iran and Afghanistan on Day +1 and continue to move eastward over Pakistan during Day +2, covering parts of northwest India.

The diagnosis of the transient weather disturbances exhibits that the reinforcement of the lower tropospheric convergence could be attributable to modulation of upper tropospheric divergence through weakening of the vertical wind shear in the westerly jet-stream. Propagation of couplet of positive and negative contours in the longitude-pressure cross sections of various terms of vorticity equation averaged over 20^{o}N-30^{o}N establishes the eastward movement of the synoptic scale transient disturbances. The vertical cross section of vorticity generation terms clearly bring out the intensification and organization of the weather system during the event day. The vorticity budget analysis of the synoptic scale system, reveal that vortex-stretching term mainly contributes to the vorticity generation, with secondary contributions from zonal at upper-tropospheric levels and meridional advection extending to lower boundary levels terms as well as the tilting term at middle-troposphere.

The divergence field mainly contributes to reinforcement of the stretching and meridional advection term, which is important for intensifying the disturbances over Saudi Arabia. Though all the terms of vorticity equation exhibit vertical variation with respect to height and westward tilt, nevertheless the stretching term exhibits stronger westward tilt over Arabian Peninsula. The southeastward propagation of the weather disturbance over Arabia is stronger at upper levels in response to the weakening of the vertical shear of the mean wind. This is balanced by the stretching term through leading the lower level trough while holding back the upper part of the trough. Further, these results are complemented by composite budget analysis of all the cases by shifting the origin of each weather disturbance to a common center (Table 2 and Figure 11). The characteristics of the Arabian weather disturbances resemble with the combination of the mid-latitude weather disturbances (Lee et. al.1988, Grotjanhn 1996, Trigo et. al. 2002) as well as the tropical weather systems (Daggupaty and Sikka 1977, Davidson

1995). The characteristics of wintertime weather disturbances, propagating from the Mediterranean region, over the wide spread Saudi Arabian desert, also are useful in exploring the dynamics of Extra-tropical and Tropical interactions. The incorporation of the convection in the vorticity equation will be helpful in exploring the transportation of sub grid-scale vorticity by convective clouds. The high-resolution data sets will be useful to further explore the meso-scale processes including the potential influences arising from the planetary boundary layer.

Acknowledgements

This research work was supported by Mitsubishi Heavy Industries/Ministry of Education (MEXT), JAPAN, Liaison Project. The constant support and encouragement received from Prof. Toshio Yamagata, Department of Earth and Planetary Science, University of Tokyo and Dr. S.K. Behera, Frontier Research System for Global Change / JAMSTEC, Tokyo, is sincerely acknowledged. The author is grateful to Dr. Tomoki Tozuka and Mr. Takafumi Miyasaka, Department of Earth and Planetary Science, University of Tokyo, for their valuable scientific and technical support throughout the study. Thanks are due to Dr. Ohba, Dr. Harada, Mr. Muta and Ms. Hoeller for their support in carrying out this research work. Thanks to Dr. R. Krishnan, IITM, for fruitful discussions and suggestions. Also critical review and constructive suggestions offered by Mr. D.R. Chakraborty, IITM were helpful in improving the manuscript. The author would like to thank Director, IITM, for enabling his visit to University of Tokyo, Japan, under the MEXT project. The publication charges for this IITM research report were met from DOD/INDOMOD/Air-Sea Project funds.

References:

Bazuhair A.S., Al-Gohani A and Sen Z., 1997: Determination of monthly wet and dry periods in Saudi Arabia. *Int. J. Climatol.*, **17**, 303-311.

Bosart, L.F. and Lin, S.C., 1984: A diagnostic analysis of the Presidents' Day storm of February 1979. *Q. J. R. Meteorol. Soc*, **112**, 2148-2177.

Chakraborty, A., Behera S.K., Mujumdar M., Ohba R., Yamagata T., 2006: Diagnosis of Tropospheric Moisture over Saudi Arabia and Influences of IOD and ENSO, *Mon. Wea. Rew.* **134**, 598-617pp.

Daggupaty S.M. and Sikka D.R., 1977: On the vorticity budget and vertical velocity distribution associated with the life cycle of a monsoon Depression, *J. Atmos. Sci.,* **34***,* 773-792.

Davidson, N.E., 1995: Vorticity budget for AMEX. Part I: Diagnostics, *Mon. Wea. Rev.*, **123**, 1620-1635.

Grotjahn R., 1996: Vorticity Equation terms for Extratropical Cyclones, *Mon. Wea. Rev.,* **124**, 2843-2858.

Holton, J.R. and Colton D.E., 1972: A diagnostic study of the vorticity balance at 200 mb. In the tropics during the northern summer. *J. Atmos. Sci.,* **29**, 1124-1128.

Hoskins, B.J. and Pedder M.A., 1980: The diagnosis of middle latitude synoptic development. *Q. J. R. Meteorol. Soc.*, **106**, 707-719.

Kalnay, E. and coauthors, 1996: The NCEP/NCAR 40 year Reanalysis Project, *Bull. Am. Meteorol. Soc.,* **77**, 437-471.

Kelin P.M., Harr P.A. and Elsbery R.L., 2002: Extratropical transition of western north Pacific tropical cyclones: Midlatitude and tropical cyclone contributions to reintensification, Mon. Wea. Rev., **130**, 2240-2259.

Krishnamurti, T.N., 1968: A diagnostic balance model for studies of weather systems of low and high latitudes, Rossby number less than 1. *Mon. Wea. Rev.,* **96**, 197-207.

Lee, T.P., Silberberg S.R. and Bosart L.F., 1988: A case study of a severe winter storm in the Middle East. *Q. J. R. Meteorol. Soc.*, **114**, 61-90.

Mayengon R., 1984: Warm core cyclones in the Mediterranean. *Mariners Weather Log*, **28**, 6-10.

Mc Toggar-Cowan R., Gyakum J.R. and Yau M.K., 2004: The impact of tropical remnants on extratropical cyclogensis : Case study of Hurricanes Danielle and Earl 1988, *Mon. Wea. Rew.*, **132**, 8, pp. 1933-1951.

Nakano, Fumitake, 2004: Fluctuations in lower troposphere associated with a quasi-stationary Rossby wave packet (A case study for 2002 summertime), Master Thesis, Available from Department of Earth and Planetary science, university of Tokyo, Japan.

Nouh, M. A., 1987: Analysis of rainfall in the south-west region of Saudi Arabia. Proc. Inst. Civ. Eng., Part 2, 339-349.

Radinoivic, D., 1987: Mediterranean cyclones and their influence on the Weather and Climate. PSMP Report Series, No. **24**, WMO, 131 pp.

Reed, R.J. and Johnson R.H., 1974: Vorticity budget of synoptic scale wave disturbances in the tropical western Pacific. J. Atmos. Sci., **31**, 1784-1790.

Reiter, E. R., 1975: 'Handbook for forecasters in the Mediterranean', Tech. Report No. 5-75. Navy Environmental Research and Prediction Facility, Monterey, California 93043.

Ritchie E.A. and Elsberry R.L., 2001: Simulations of the transformation stage of the extratropical transition of tropical cyclones. Mon. Wea. Rev., **129**, 1462-1480.

Sen, Z., 1983: 'Hydrology of Saudi Arabia', Symposium on Water Resources in Saudi Arabia, Management, Treatment and Utilization, Riyadh. pp 68-94.

Trigo I. F., Bigg G. R. and Davis T. D., 2002: Climatology of cyclogenesis mechanisms in the Mediterranean. Mon. Wea. Rev., **130**, 549-569.

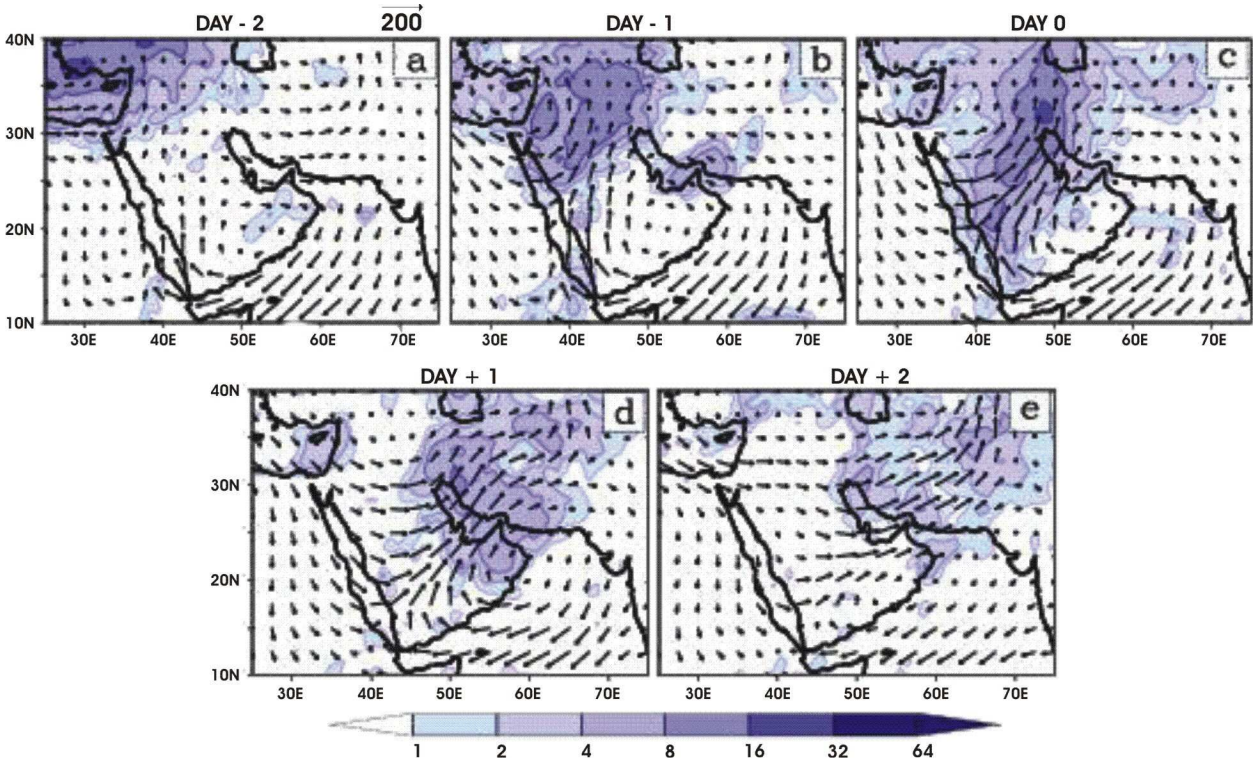

Figure 1. Time sequence of composited daily rainfall and moisture transport showing the evolution of Arabian rainfall events during January : a) for Day -2, b) for Day -1, c) for Day 0, d) for Day +1, e) for Day +2. The shading represents rainfall (units : mm/day), zero contour is suppressed. Moisture transport vector $\vec{Q}$ (units: Kg m^{-1} s^{-1}).

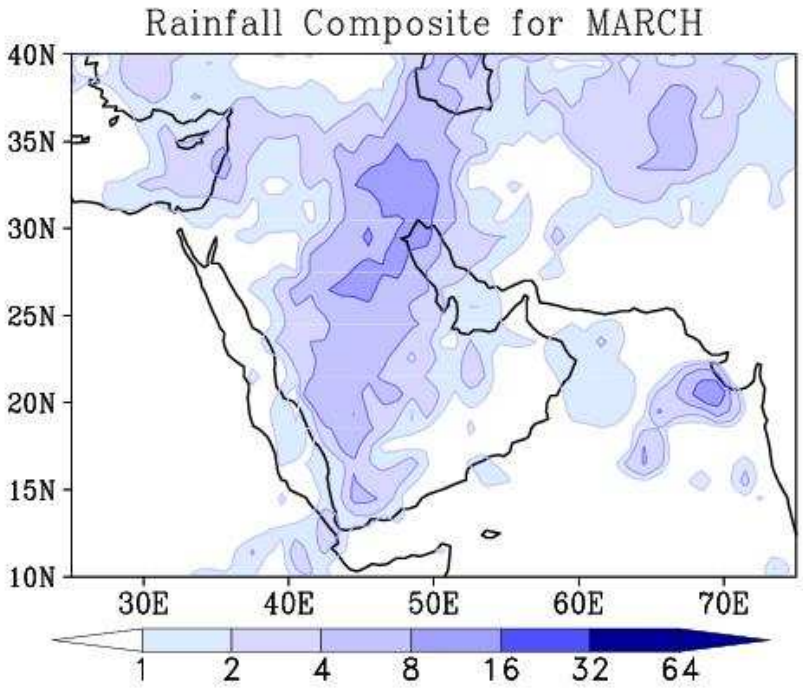

Figure 2. Composite map of Arabian rainfall events during March. The shading represents the rainfall (units: mm/day), zero contour is suppressed.

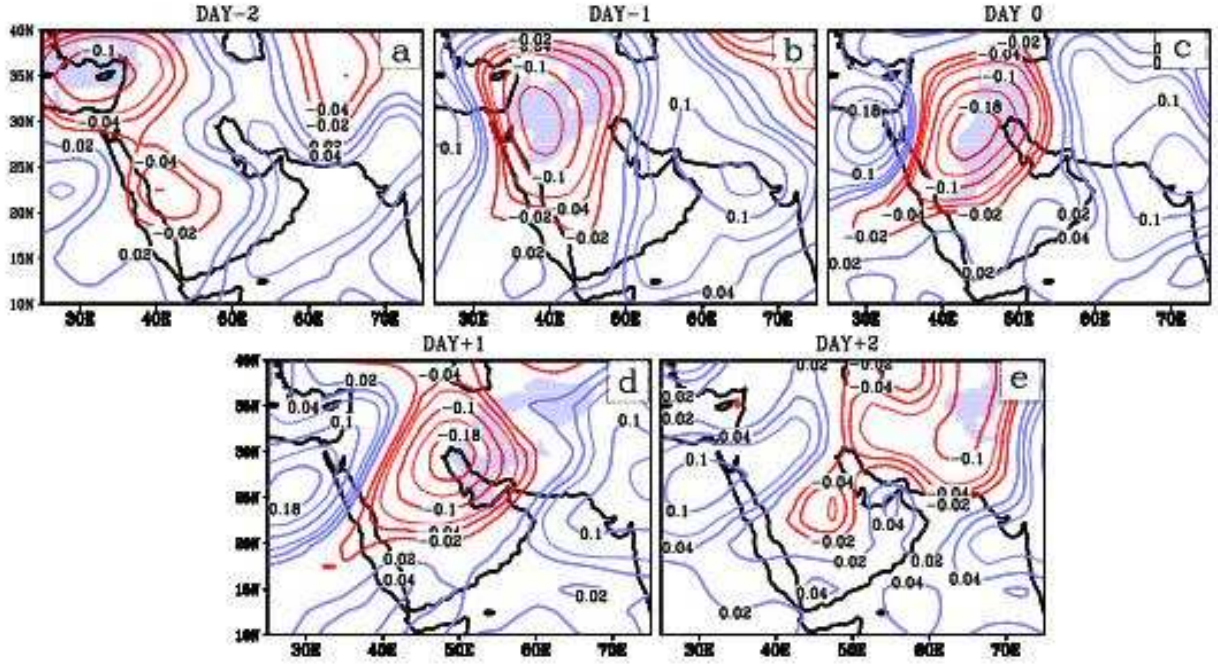

Figure 3. Same as Figure 1 except for vertical velocity (units: Pa s^{-1}) at 500 hPa. The contour interval is 0.02 units and zero contour is suppressed. The light shading represents statistical significance, of mid-tropospheric vertical velocity patterns, exceeding 90% level.

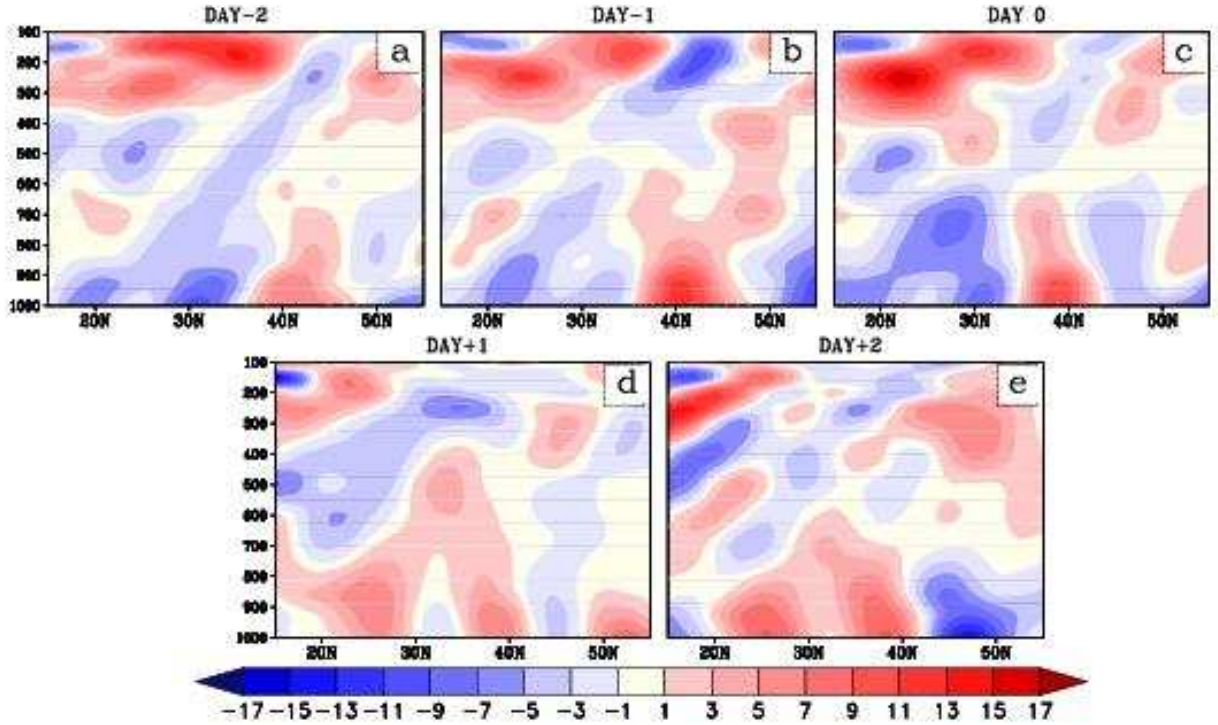

Figure 4. Same as Figure 1 except for the Latitude-pressure cross section of horizontal wind divergence (units: 10^{-6} s^{-1}). The contour interval is 2 units and zero contour is suppressed.

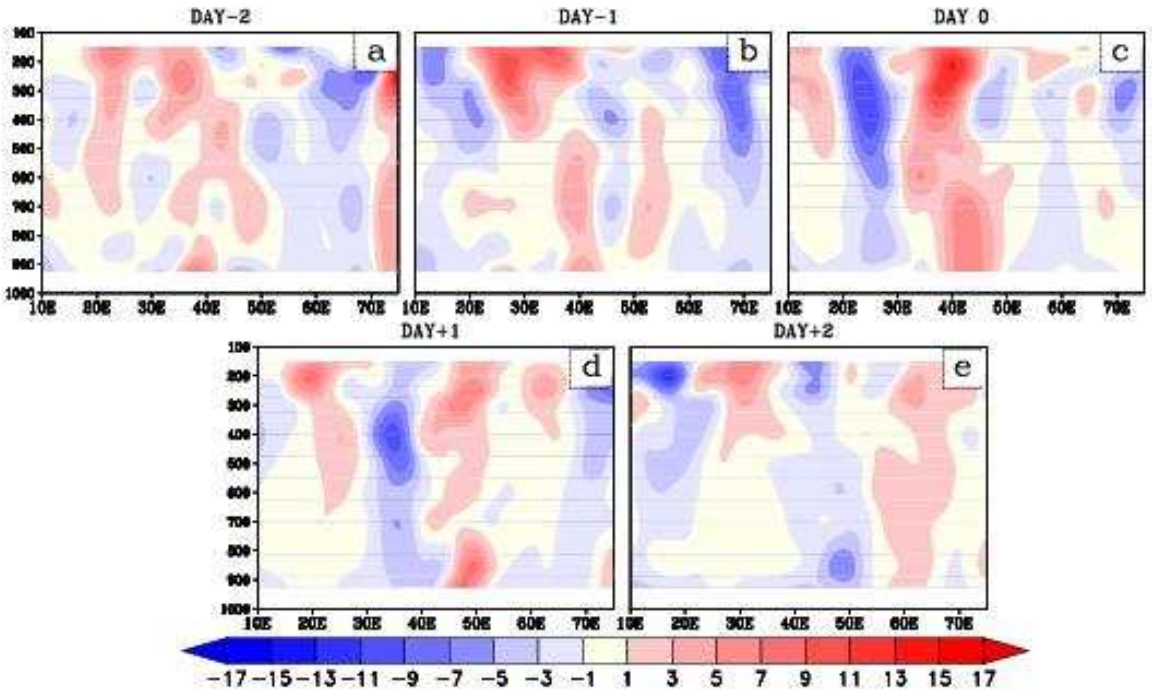

Figure 5. The vertical cross section of time sequence of the local rate of change of vorticity due to all the large-scale terms in the vorticity equation (described in the text) for a typical event of 8 January 1999 : a) for 6 January, b) for 7 January, c) for 8 January, d) for 9 January and e) for 10 January. The computed quantities are averaged over 20 - 30^0 N and displayed in longitude-pressure plane. The shading represents the tendency terms (Units: $10^{-11}s^{-2}$) in the vorticity equation, contour interval is 2 units and zero contour is suppressed.

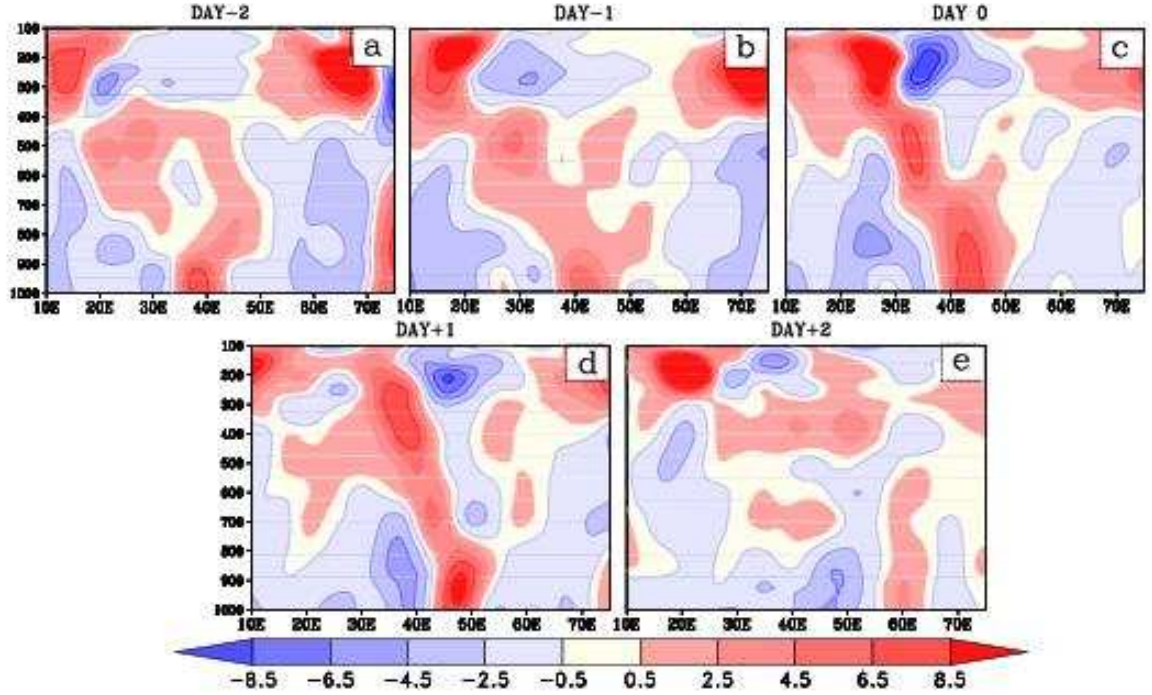

Figure 6. Same as Figure 5 except for the Stretching term in the vorticity equation.

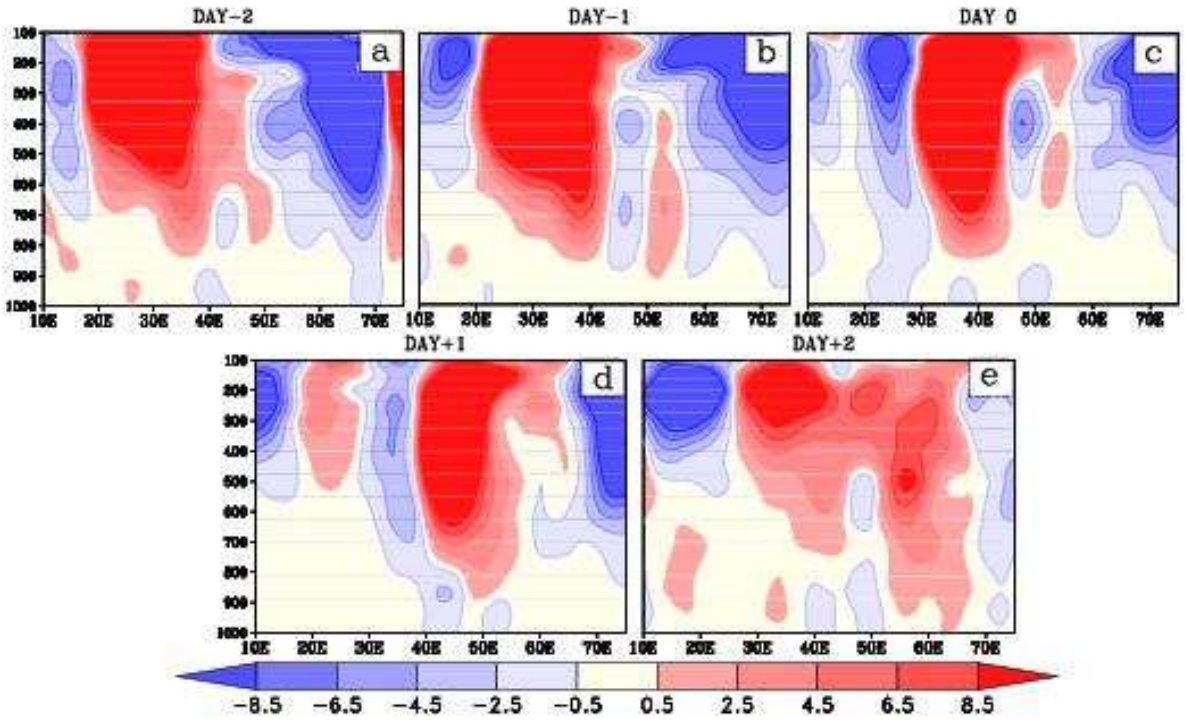

Figure 7. Same as Figure 5 except for the zonal advection term in the vorticity equation.

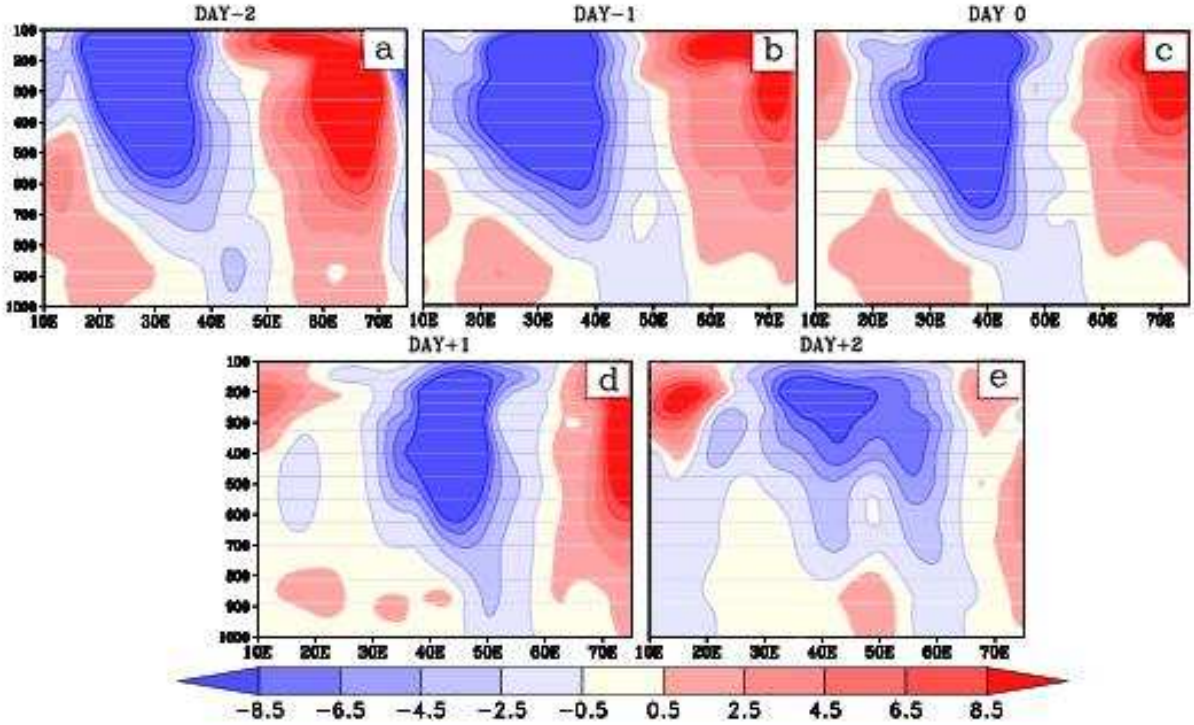

Figure 8. Same as Figure 5 except for the meridional advection term in the vorticity equation.

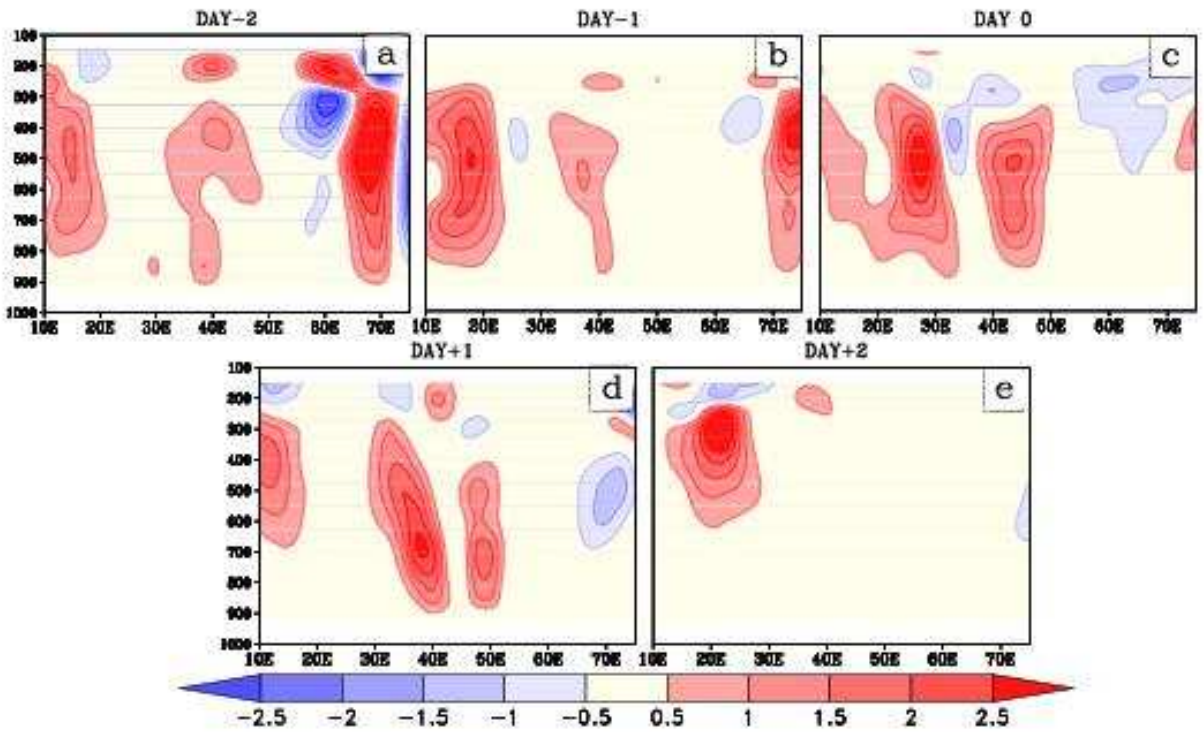

Figure 9. Same as Figure 5 except for the vertical advection term in the vorticity equation.

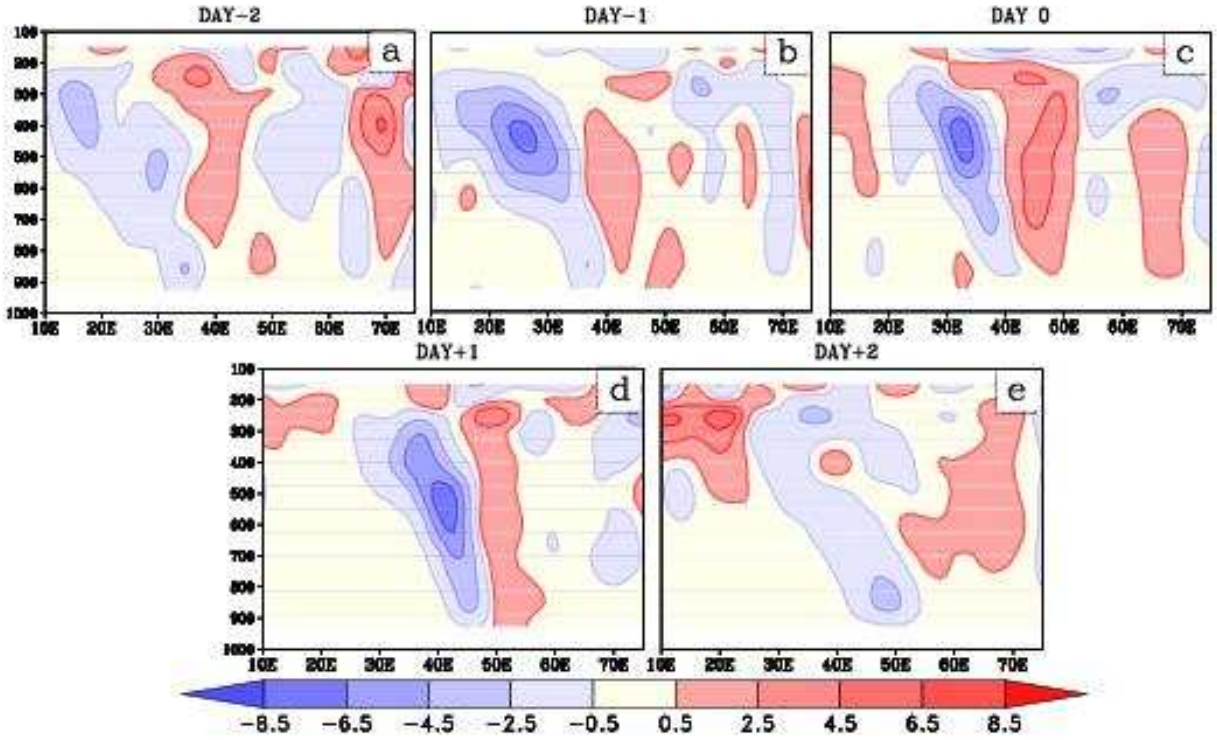

Figure 10. Same as Figure 5 except for the tilting term in the vorticity equation.

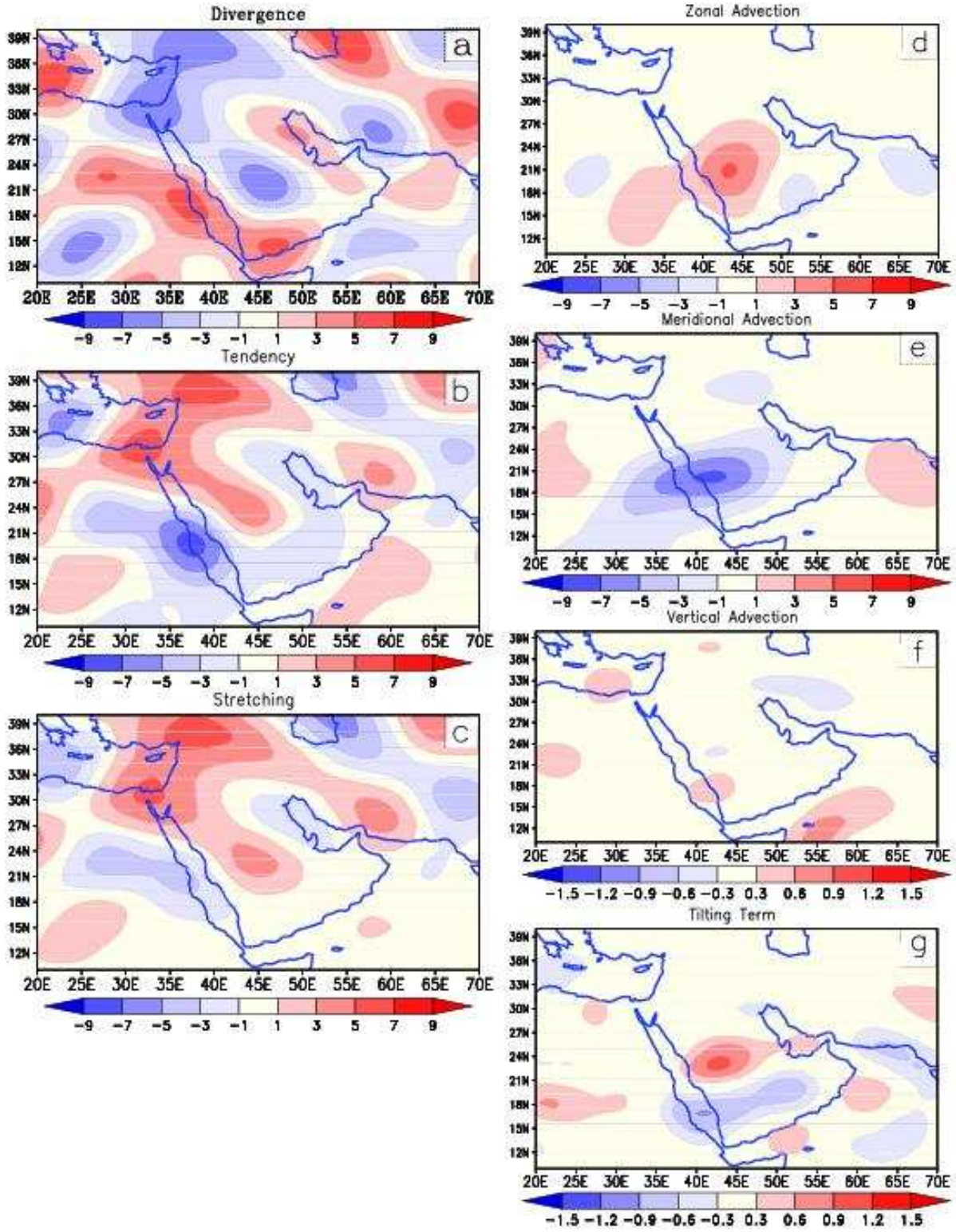

Figure 11. a) Composite of horizontal divergence (units: 10^{-6} s^{-1}) at 700 hPa. Composite maps showing terms in the vorticity equation at 700 hPa (units: 10^{-11} s^{-2}) b) Tendency c) Stretching d) Zonal advection e) Meridional advection f) Vertical advection g) Tilting term. The composite is based on the significant Arabian rainfall events of January. The data for each case were shifted so as to place the center of weather disturbance at (20^{o}N, 43^{o}E).

I. I. T. M. RESEARCH REPORTS

- Energetic consistency of truncated models, Asnani G.C., August 1971, RR-001.
- Note on the turbulent fluxes of heat and moisture in the boundary layer over the Arabian Sea, Sinha S., August 1971, RR-002.
- Simulation of the spectral characteristics of the lower atmosphere by a simple electrical model and using it for prediction, Sinha S., September 1971, RR-003.
- Study of potential evapo-transpiration over Andhra Pradesh, Rakhecha P.R., September 1971, RR-004.
- Climatic cycles in India-1: Rainfall, Jagannathan P. and Parthasarathy B., November 1971, RR-005.
- Tibetan anticyclone and tropical easterly jet, Raghavan K., September 1972, RR-006.
- Theoretical study of mountain waves in Assam, De U.S., February 1973, RR-007.
- Local fallout of radioactive debris from nuclear explosion in a monsoon atmosphere, Saha K.R. and Sinha S., December 1972, RR-008.
- Mechanism for growth of tropical disturbances, Asnani G.C. and Keshavamurty R.N., April 1973, RR-009.
- Note on “Applicability of quasi-geostrophic barotropic model in the tropics”, Asnani G.C., February 1973, RR-010.
- On the behaviour of the 24-hour pressure tendency oscillations on the surface of the earth, Part-I: Frequency analysis, Part-II: Spectrum analysis for tropical stations, Misra B.M., December 1973, RR-011.
- On the behaviour of the 24 hour pressure tendency oscillations on the surface of the earth, Part-III : Spectrum analysis for the extra-tropical stations, Misra B.M., July 1976, RR-011A.
- Dynamical parameters derived from analytical functions representing Indian monsoon flow, Awade S.T. and Asnani G.C., November 1973, RR-012.
- Meridional circulation in summer monsoon of Southeast Asia, Asnani G.C., November 1973, RR-014.
- Energy conversions during weak monsoon, Keshavamurty R.N. and Awade S.T., August 1974, RR-015.
- Vertical motion in the Indian summer monsoon, Awade S.T. and Keshavamurty R.N., August 1974, RR-016.
- Semi-annual pressure oscillation from sea level to 100mb in the northernhemisphere, Asnani G.C. and Verma R.K., August 1974, RR-017.
- Suitable tables for application of gamma probability model to rainfall, Mooley D.A., November 1974, RR-018.

- Annual and semi-annual thickness oscillation in thenorthern hemisphere, Asnani G.C. and Verma R.K., January 1975, RR-020.

- Spherical harmonic analysis of the normal constant pressure charts in the northern hemisphere, Awade S.T., Asnani G.C. and Keshavamurty R.N., May 1978, RR-021.

- Dynamical parameters derived from analytical function representing normal July zonal flow along 87.5 °E, Awade S.T. and Asnani G.C., May 1978, RR-022.

- Study of trends and periodicities in the seasonal and annual rainfall of India, Parthasarathy B. and Dhar O.N., July 1975, RR-023.

- Southern hemisphere influence on Indian rainfall, Raghavan K.., Paul D.K. and Upasani P.U., February 1976, RR-024.

- Climatic fluctuations over Indian region - Rainfall : A review, Parthasarathy B. and Dhar O.N., May 1978, RR-025.

- Annual variation of meridional flux of sensible heat, Verma R.K. and Asnani G.C., December 1978, RR-026.

- Poisson distribution and years of bad monsoon over India, Mooley D.A and Parthasarathy B., April 1980, RR-027.

- On accelerating the FFT of Cooley and Tukey, Mishra S.K., February 1981, RR-028.

- Wind tunnel for simulation studies of the atmospheric boundary layer, Sivaramakrishnan S., February 1981, RR-029.

- Hundred years of Karnataka rainfall, Parthasarathy B. and Mooley D.A., March 1981, RR-030.

- Study of the anomalous thermal and wind patterns during early summer season of 1979 over the Afro-Asian region in relation to the large-scale performance of the monsoon over India, Verma R.K. and Sikka D.R., March 1981, RR-031.

- Some aspects of oceanic ITCZ and its disturbances during the onset and established phase of summer monsoon studied with Monex-79 data, Sikka D.R., Paul D.K. and Singh S.V., March 1981, RR- 032.

- Modification of Palmer drought index, Bhalme H.N. and Mooley D.A., March 1981, RR-033.

- Meteorological rocket payload for Menaka-II/Rohini 200 and its developmental details, Vernekar K.G. and Brij Mohan, April 1981, RR-034.

- Harmonic analysis of normal pentad rainfall of Indian stations, Anathakrishnan R. and Pathan J.M., October 1981, RR-035.

- Pentad rainfall charts and space-time variations of rainfall over India and the adjoining areas, Anathakrishnan R. and Pathan J.M., November 1981, RR-036.

- Dynamic effects of orography on the large scale motion of the atmosphere Part I : Zonal flow and elliptic barrier with maximum height of one km., Bavadekar S.N. and Khaladkar R.M., January 1983, RR-037.

- Limited area five level primitive equation model, Singh S.S., February 1983, RR-038.

- Developmental details of vortex and other aircraft thermometers, Vernekar K.G., Brij Mohan and Srivastava S., November 1983, RR-039.

- Note on the preliminary results of integration of a five level P.E. model with westerly wind and low orography, Bavadekar S.N., Khaladkar R.M., Bandyopadhyay A. and Seetaramayya P., November 1983, RR-040.
- Long-term variability of summer monsoon and climatic change, Verma R.K., Subramaniam K. and Dugam S.S., December 1984, RR-041.

- Project report on multidimensional initialization for NWP models, Sinha S., February 1989, RR-042.

- Numerical experiments with inclusion of orography in five level P.E. Model in pressure-coordinates for interhemispheric region, Bavadekar S.N. and Khaladkar R.M., March 1989, RR-043.

- Application of a quasi-lagrangian regional model for monsoon prediction, Singh S.S. and Bandyopadhyay A., July 1990, RR-044.

- High resolution UV-visible spectrometer for atmospheric studies, Bose S., Trimbake H.N., Londhe A.L. and Jadhav D.B., January 1991, RR-045.

- Fortran-77algorithm for cubic spline interpolation for regular and irregular grids, Tandon M.K., November 1991, RR-046.

- Fortran algorithm for 2-dimensional harmonic analysis, Tandon M.K., November 1991, RR- 047.

- 500 hPa ridge and Indian summer monsoon rainfall : A detailed diagnostic study, Krishna Kumar K., Rupa Kumar K. and Pant G.B., November 1991, RR-048.

- Documentation of the regional six level primitive equation model, Singh S.S. and Vaidya S.S., February 1992, RR-049.

- Utilisation of magnetic tapes on ND-560 computer system, Kripalani R.H. and Athale S.U., July 1992, RR-050.

- Spatial patterns of Indian summer monsoon rainfall for the period 1871-1990, Kripalani R.H., Kulkarni A.A., Panchawagh N.V. and Singh S.V., August 1992, RR-051.

- FORTRAN algorithm for divergent and rotational wind fields, Tandon M.K., November 1992, RR-052.

- Construction and analysis of all-India summer monsoon rainfall series for the longest instrumental period: 1813-1991, Sontakke N.A., Pant G.B. and Singh N., October 1992, RR-053.

- Some aspects of solar radiation, Tandon M.K., February 1993, RR-054.

- Design of a stepper motor driver circuit for use in the moving platform, Dharmaraj T. and Vernekar K.G., July 1993, RR-055.

- Experimental set-up to estimate the heat budget near the land surface interface, Vernekar K.G., Saxena S., Pillai J.S., Murthy B.S., Dharmaraj T. and Brij Mohan, July 1993, RR-056.

- Identification of self-organized criticality in atmospheric total ozone variability, Selvam A.M. and Radhamani M., July 1993, RR-057.

- Deterministic chaos and numerical weather prediction, Selvam A.M., February 1994, RR-058.

- Evaluation of a limited area model forecasts, Singh S.S., Vaidya S.S Bandyopadhyay A., Kulkarni A.A, Bawiskar S.M.,Sanjay J., Trivedi D.K. and Iyer U., October 1994, RR-059.

- Signatures of a universal spectrum for atmospheric interannual variability in COADS temperature time series, Selvam A.M., Joshi R.R. and Vijayakumar R., October 1994, RR-060.
- Identification of self-organized criticality in the interannual veriability of global surface temperature, Selvam A.M. and Radhamani M., October 1994, RR-061.

- Identification of a universal spectrum for nonlinear veriability of solar-geophysical parameters, Selvam A.M., Kulkarni M.K., Pethkar J.S. and Vijayakumar R., October 1994, RR-062.

- Universal spectrum for fluxes of energetic charged particles from the earth's magnetosphere, Selvam A.M. and Radhamani M., June 1995, RR-063.

- Estimation of nonlinear kinetic energy exchanges into individual triad interactions in the frequency domain by use of the cross-spectral technique, Chakraborty D.R., August 1995, RR-064.

- Monthly and seasonal rainfall series for all-India homogeneous regions and meteorological subdivisions: 1871-1994, Parthasarathy B., Munot A.A. and Kothawale D.R., August 1995, RR-065.

- Thermodynamics of the mixing processes in the atmospheric boundary layer over Pune during summer monsoon season, Morwal S.B. and Parasnis S.S., March 1996, RR-066.

- Instrumental period rainfall series of the Indian region: A documentation, Singh N. and Sontakke N.A., March 1996, RR-067.

- Some numerical experiments on roundoff-error growth in finite precision numerical computation, Fadnavis S., May 1996, RR-068.

- Fractal nature of MONTBLEX time series data, Selvam A.M. and Sapre V.V., May 1996, RR-069.

- Homogeneous regional summer monsoon rainfall over India: Interannual variability and teleconnections, Parthasarathy B., Rupa Kumar K. and Munot A.A., May 1996, RR-070.

- Universal spectrum for sunspot number variability, Selvam A.M. and Radhamani M., November 1996, RR-071.

- Development of simple reduced gravity ocean model for the study of upper north Indian Ocean, Behera S.K. and Salvekar P.S., November 1996, RR-072.

- Study of circadian rhythm and meteorological factors influencing acute myocardial infraction, Selvam A.M., Sen D. and Mody S.M.S., April 1997, RR-073.

- Signatures of universal spectrum for atmospheric gravity waves in southern oscillation index time series, Selvam A.M., Kulkarni M.K., Pethkar J.S. and Vijayakumar R., December 1997, RR-074.

- Some example of X-Y plots on Silicon Graphics, Selvam A.M., Fadnavis S. and Gharge S.P., May 1998, RR-075.

- Simulation of monsoon transient disturbances in a GCM, Ashok K., Soman M.K. and Satyan V., August 1998, RR-076.

- Universal spectrum for intraseasonal variability in TOGA temperature time series, Selvam A.M., Radhamani M., Fadnavis S. and Tinmaker M.I.R., August 1998, RR-077.

- One dimensional model of atmospheric boundary layer, Parasnis S.S., Kulkarni M.K., Arulraj S. and Vernekar K.G., February 1999, RR-078.

- Diagnostic model of the surface boundary layer - A new approach, Sinha S., February 1999, RR-079.
- Computation of thermal properties of surface soil from energy balance equation using force - restore method, Sinha S., February 1999, RR-080.
- Fractal nature of TOGA temperature time series, Selvam A.M. and Sapre V.V., February 1999, RR-081.
- Evolution of convective boundary layer over the Deccan Plateau during summer monsoon, Parasnis S.S., February 1999, RR-082.
- Self-organized criticality in daily incidence of acute myocardial infarction, Selvam A.M., Sen D., and Mody S.M.S., Feburary 1999, RR-083.
- Monsoon simulation of 1991 and 1994 by GCM : Sensitivity to SST distribution, Ashrit R.G., Mandke S.K. and Soman M.K., March 1999, RR-084.
- Numerical investigation on wind induced interannual variability of the north Indian Ocean SST, Behera S.K., Salvekar P.S. and Ganer D.W., April 1999, RR-085.
- On step mountain eta model, Mukhopadhyay P., Vaidya S.S., Sanjay J. and Singh S.S., October 1999, RR-086.
- Land surface processes experiment in the Sabarmati river basin: an overview and early results, Vernekar K.G., Sinha S., Sadani L.K., Sivaramakrishnan S., Parasnis S.S., Brij Mohan, Saxena S., Dharamraj T., Pillai, J.S., Murthy B.S., Debaje, S.B., Patil, M.N. and Singh A.B., November 1999, RR-087.
- Reduction of AGCM systematic error by Artificial Neural Network: A new approach for dynamical seasonal prediction of Indian summer monsoon rainfall, Sahai A.K. and Satyan V., December 2000, RR-088.
- Ensemble GCM simulations of the contrasting Indian summer monsoons of the 1987 and 1988, Mujumdar M. and Krishnan R., February 2001, RR-089.
- Aerosol measurements using lidar and radiometers at Pune during INDOEX field phases, Maheskumar R.S., Devara P.C.S., Raj P.E., Jaya Rao Y., Pandithurai G., Dani K.K., Saha S.K., Sonbawne S.M. and Tiwari Y.K., December 2001, RR-090.
- Modelling studies of the 2000 Indian summer monsoon and extended analysis, Krishnan R., Mujumdar M., Vaidya V., Ramesh K.V. and Satyan V., December 2001, RR-091.
- Intercomparison of Asian summer monsoon 1997 simulated by atmospheric general circulation models, Mandke S.K., Ramesh K.V. and Satyan V., December 2001, RR-092.
- Prospects of prediction of Indian summer monsoon rainfall using global SST anomalies, Sahai A.K, Grimm A.M., Satyan V. and Pant G.B., April 2002, RR-093.
- Estimation of nonlinear heat and momentum transfer in the frequency domain buy the use of frequency co-spectra and cross-bispectra, Chakraborty D.R. and Biswas M.K., August 2002, RR-094
- Real time simulations of surface circulations by a simple ocean model, Reddy P.R.C., Salvekar P.S., Ganer D.W. and Deo A.A., January 2003, RR-095

- Evidence of twin gyres in the Indian ocean : new insights using reduced gravity model by daily winds, Reddy P.R.C., Salvekar P.S., Ganer D.W. and Deo A.A., February 2003, RR-096

- Dynamical seasonal prediction experiments of the Indian summer monsoon, Mujumdar M., Krishnan R. and Satyan V., June 2003, RR-097

- Thermodynamics and dynamics of the upper ocean mixed layer in the central and eastern Arabian Sea, Gnanaseelan C., Mishra A.K., Thompson B. and. Salvekar P.S, August 2003, RR-098
- Measurement of profiles and surface energy fluxes on the west coast of India at Vasco-Da-Gama, Goa during ARMEX 2002-03, Sivaramakrishnan S., Murthy B.S., Dharamraj T., Sukumaran C. and Rajitha Madhu Priya T., August 2003, RR-099

- Time – mean oceanic response and interannual variability in a global ocean GCM simulation, Ramesh K.V. and Krishnan R., September 2003, RR-100

- Multimodel scheme for prediction of monthly rainfall over India, Kulkarni J.R., Kulkarni S.G., Badhe Y., Tambe S S., Kulkarni B.D. and Pant G.B., December 2003, RR-101

- Mixed layer and thermocline interactions associated with monsoonal forcing over the Arabian Sea, Krishnan R. and Ramesh K.V., January 2004, RR-102

- Interannual variability of Kelvin and Rossby waves in the Indian Ocean from TOPEX/ POSEIDON altimetry data, Gnanaseelan C., Vaid B.H., Polito P.S. and Salvekar P.S., March 2004, RR-103

- Initialization experiments over Indian region with a limited area model using recursive digital filters, Badyopadhyay S. and Mahapatra S., July 2004, RR-104

- Sensitivity of Indian monsoon rainfall to different convective parameters in the relaxed Arakawa-Schubert scheme, Pattanaik D.R. and Satyan V., October 2004, RR-105

- Simulation of tropical Indian ocean surface circulation using a free surface sigma coordinate model, Prem Singh and Salvekar P.S., December 2004, RR-106

- Dynamical ensemble seasonal forecast experiments of recent Indian summer monsoons : an assessment using new approach, Mandke S.K., Sahai A.K. and Shinde M.A., July 2005, RR-107

- Indian Ocean Dipole simulation using modular ocean model, Thompson B., Gnanaseelan C. and Salvekar P.S., July 2005, RR-108

- Influence of El Nino on the biennial and annual Rossby waves propagation in the Indian Ocean with special emphasis on Indian Ocean Dipole, Vaid B.H., Gnanaseelan C., Polito* P.S. and Salvekar P.S., January 2006, RR-109

- A Model study of Indian summer monsoon drought of 2002: Influence of tropical convective activity over northwest Pacific, Vinay Kumar, Krishnan R. and Mujumdar Milind, April 2006, RR-110